

## Supplementary Information

### Unconventional Organic Solar Cell Structure Based on Hyperbolic Metamaterial

Yu-Chieh Chao<sup>a</sup>, Hung-I Lin<sup>b</sup>, Jia-Yu Lin<sup>a</sup>, Yu-Chuan Tsao<sup>a</sup>, Yu-Ming Liao<sup>b,c</sup>, Fang-Chi Hsu<sup>d\*</sup> and Yang-Fang Chen<sup>a,e\*</sup>

<sup>a</sup>Department of Physics, National Taiwan University, Taipei 106, Taiwan

<sup>b</sup>Department of Materials Science and Engineering, Massachusetts Institute of Technology, 77 Massachusetts Avenue, Cambridge, MA 02139, USA

<sup>c</sup>Nano-Science and Technology Program, Taiwan International Graduate Program, Academia Sinica, Taipei 115, Taiwan

<sup>d</sup>Department of Materials Science and Engineering, National United University, Miaoli 360, Taiwan

<sup>e</sup>Advanced Research Centre for Green Materials Science and Technology, National Taiwan University, Taipei 106, Taiwan

\*Authors to whom correspondence should be addressed.

*E-mail addresses:* fangchi@nuu.edu.tw (F. C. Hsu); yfchen@phys.ntu.edu.tw (Y. F. Chen)

## S1. Sample structures for photoluminescence (PL) measurements and Simulation

Both samples were prepared on Si wafers. For PL measurements, the light was incident on the P3HT:PCBM side. In simulation, the 0 point in the z-axis is at the top surface of the substrates with incident light along the negative z-direction, as shown in Fig. S1.

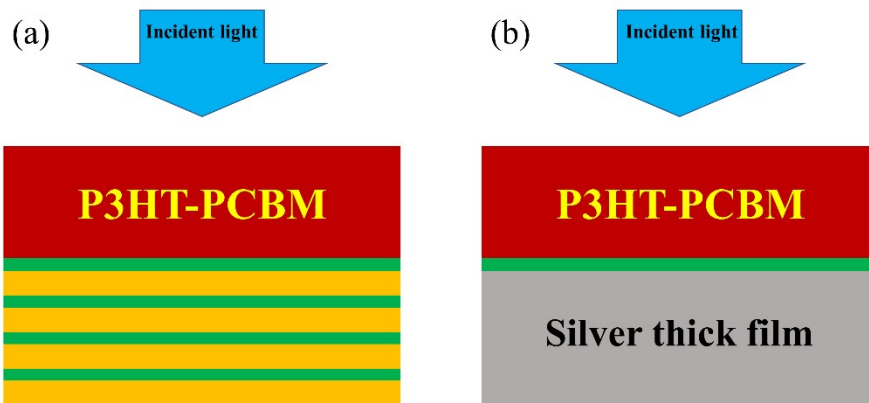


**Figure S1. Schematic illustration of samples for PL measurements and FDTD simulation.** The samples structures for (a) HMM and (b) MoO<sub>3</sub>/Ag structures on Si wafers.

## S2. Hyperbolic-dispersion calculations.

To derive the dispersion behavior of multilayer structures, the calculation of effective dielectric tensors based on the effective medium theory (EMT) is provided as follows. Because the thicknesses of Au (25 nm) and MoO<sub>3</sub> (7 nm) layers are much smaller than the wavelength of the incident light, the effective permittivity tensor can be considered homogeneous. Therefore, the dielectric tensor components parallel ( $\varepsilon_{\parallel}$ ) and perpendicular ( $\varepsilon_{\perp}$ ) to the surface of HMM are determined as:<sup>1</sup>

$$\varepsilon_{\parallel} = \varepsilon_x = \varepsilon_y = \sum_{n=1}^2 f_n \varepsilon_n \quad (\text{S1})$$

$$\varepsilon_{\perp}^{-1} = \varepsilon_z^{-1} = \sum_{n=1}^2 f_n \varepsilon_n^{-1} \quad (\text{S2})$$

$$f_n = \frac{d_n}{\sum_{n=1}^2 d_n} \quad (\text{S3})$$

where  $f_n$  is the fill fraction of the layer component,  $\varepsilon_n$  is the permittivity, and  $d_n$  is the thickness of the  $n$ th layer of the multilayer structure. Denoting  $n = \text{metal } (m)$  and dielectric ( $d$ ) here, the dielectric tensor components are given by:

$$\varepsilon_{\parallel} = \rho \varepsilon_m + (1 - \rho) \varepsilon_d \quad (\text{S4})$$

and

$$\varepsilon_{\perp} = \frac{\varepsilon_m \varepsilon_d}{\rho \varepsilon_d + (1 - \rho) \varepsilon_m} \quad (\text{S5})$$

where  $\rho$  is the fill fraction of the metal component in the stack of the multilayer structure.

For hyperbolic dispersion relation of HMM,  $\varepsilon_{\perp} \cdot \varepsilon_{\parallel} < 0$ ; otherwise,  $\varepsilon_{\perp} \cdot \varepsilon_{\parallel} > 0$  for elliptical or spherical dispersion. Fig. S2 shows the calculation results for effective permittivity components of the designed HMM as function of wavelength. It is found

that for wavelength ( $\lambda$ )  $\leq 420$  nm (green region),  $\varepsilon_{\perp} \cdot \varepsilon_{\parallel} > 0$  whereas  $\varepsilon_{\perp} \cdot \varepsilon_{\parallel} < 0$  for  $\lambda \geq 420$  nm (orange region). It is known that the iso-frequency surface of a propagating wave is given by:<sup>2,3</sup>

$$\frac{\omega^2}{c^2} = \frac{k_x^2 + k_y^2}{\varepsilon_{\perp}} + \frac{k_z^2}{\varepsilon_{\parallel}}, \quad (\text{S6})$$

where  $\omega$  is the angular frequency;  $k_x$ ,  $k_y$ , and  $k_z$  are the components of the wave vector along x, y, and z-axis, respectively; x and y are directions parallel to the HMM surface while z-direction is perpendicular to the HMM layer; c is the speed of light in vacuum. The green region ( $\lambda \leq 420$  nm) corresponds to an elliptical iso-frequency surface ( $\varepsilon_{\perp} \cdot \varepsilon_{\parallel} > 0$ ) and the orange region ( $\lambda \geq 420$  nm) is a hyperboloid ( $\varepsilon_{\perp} \cdot \varepsilon_{\parallel} < 0$ ).

To further confirm the designed HMM achieving hyperbolic dispersion, we also calculated the effective permittivity from the optical characteristics (*i.e.*, transmission (T), reflection (R), and absorption (A) spectra). For a wave propagating inside a layered structure, the complex effective refractive indices ( $n + ik$ ) can also be realized via absorption (A) spectrum using the incoherent interference formula in a slab.<sup>4</sup> Both  $n$  and  $k$  can be retrieved from the T and R spectra as:

$$n = \frac{(1 + R_{ah})}{(1 - R_{ah})} - \left[ \frac{4R_{ah}}{(1 - R_{ah})^2} - k^2 \right]^{\frac{1}{2}} \quad (\text{S7})$$

$$\text{and } k = \frac{-\lambda}{4\pi t} \ln \left\{ \frac{[T^2 - (1 - R)^2] + \{[T^2 - (1 - R)^2]^2 + 4T^2\}^{\frac{1}{2}}}{2T} \right\} \quad (\text{S8})$$

$$\text{where } R_{ah} = \frac{R}{1 + \frac{[T^2 - (1 - R)^2] + \{[T^2 - (1 - R)^2]^2 + 4T^2\}^{\frac{1}{2}}}{2}} \quad (\text{S9})$$

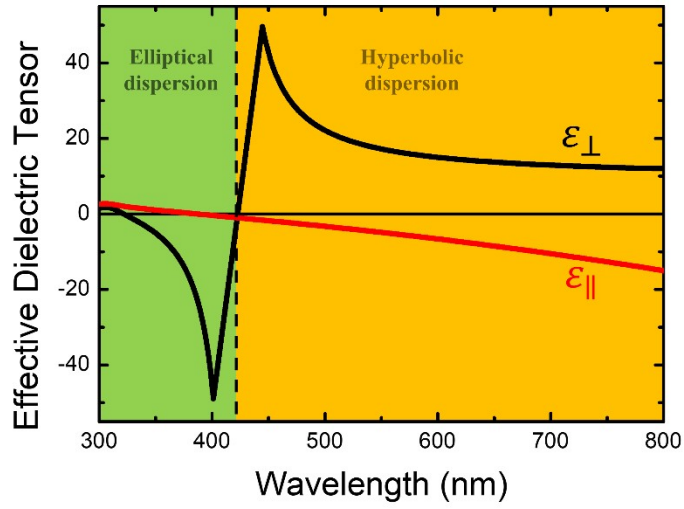
where  $R_{ah}$  is the surface reflectance between air and HMM substrate and  $t$  is the thickness of the layer. In this simulation method, the permeability is unchanged because of not introducing any magnetic materials in this work. Thus, the effective permittivity is subsequently determined:

$$\varepsilon_y^{eff} = (n + ik)^2 \quad (S10)$$

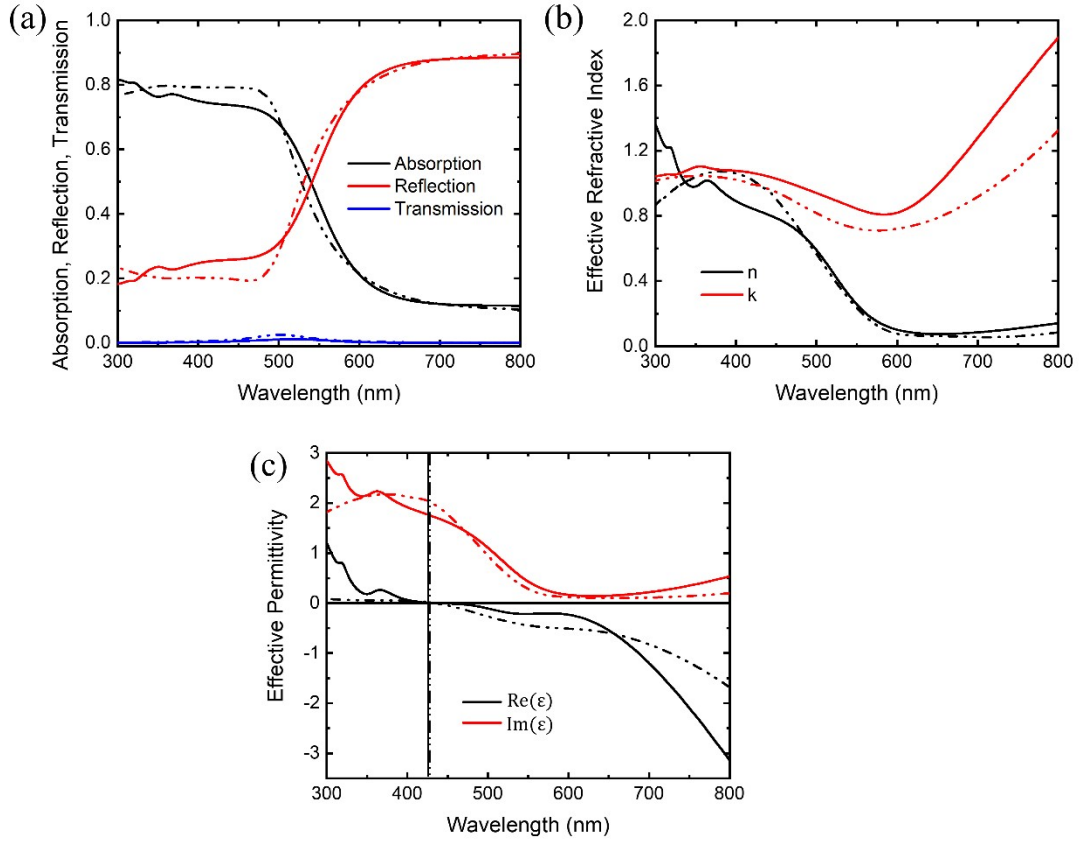
Fig. S3a shows T, R, and A spectra of the designed HMM substrate obtained from using the three-dimensional (3D) finite-difference time-domain (FDTD) technique (—) and experimental measurements (-·-). Fig. S3b presents the retrieved complex reflective indices  $n$  and  $k$  for the designed HMM structure for the values taken from simulated optical spectra (—) and experimental obtained spectra (-·-) in Fig. S3a. Based on the retrieved complex reflective indices, one can calculate the corresponding real and imaginary parts of the effective permittivity  $\varepsilon_y^{eff}$  as the results for simulated optical spectra (—) and measured spectra (-·-) shown in Fig. S3c. The transition wavelengths of iso-frequency surfaces can be obtained at 433 and 435 nm for simulated and measured optical spectra, respectively, a result which quite agrees with each other and is very close to 420 nm yielded in Fig. S2.

Fig. S2 is obtained from the effective medium theory (EMT) while Fig. S3c is calculated based on the transmission and reflection spectra yielded from FDTD simulation and HMM sample measurements. In the EMT, only the dielectric constant of each component and their thickness ratio are considered. Parameters related to sample thickness such as the real thickness of each component and the number of metal/dielectric pairs are not included in the calculation. Therefore, one can only gain the fundamental information about wavelength region for hyperbolic dispersion of a HMM structure. The real value of  $\varepsilon_{||}$  might not be accurate. On the other hand, to retrieve the effective permittivity from the optical characteristics, the optical spectra can be obtained experimentally and the resulting spectra carry the information about the physical properties of a HMM structure. Thus, the total thickness or the pair numbers of the HMM structure is involved in the retrieval procedure. In this approach, the obtained value of  $\varepsilon_{||}$  is expected to be more close to the real value. Though both methods

have discrepancy in the value of  $\epsilon_{\parallel}$ , the predicted wavelength region for hyperbolic dispersion of a HMM structure agrees with each other very well.



**Figure S2. Hyperbolic-dispersion calculations.** The effective dielectric tensor calculation for the designed HMM. Green region ( $\lambda \leq 420$  nm) is the elliptical dispersion ( $\epsilon_{\perp} \cdot \epsilon_{\parallel} > 0$ ) and orange region ( $\lambda \geq 420$  nm) is the hyperbolic dispersion ( $\epsilon_{\perp} \cdot \epsilon_{\parallel} < 0$ ).



**Figure S3. Optical properties of HMM substrates.** (a) Absorption, reflection and transmission spectra of designed HMM obtained from FDTD technique (—) and experimental measurements (---). (b) The complex refractive indices,  $n$  and  $k$ , calculated from FDTD obtained (—) and measured (---) transmission and reflection spectra. (c) Real and imaginary parts of the effective permittivity,  $\epsilon_y^{eff} = (n + ik)^2$  obtained from simulated (—) and measured (---) optical spectra.

### S3. The cut-off wave-vectors spectrum

The cutoff wave-vectors for the designed HMM in visible light regime can be

determined by  $\frac{k_{cutoff}}{k_0} = \pm \sqrt{\frac{(1 + \eta)\epsilon_m\epsilon_d}{\epsilon_m + \eta\epsilon_d}}$ , where  $\eta$  is the filling factor,  $\epsilon_m$  is the permittivity of metal, and  $\epsilon_d$  is the permittivity of dielectric.<sup>5</sup> The calculated cut-off

wave vector spectrum is presented in Fig. S4.

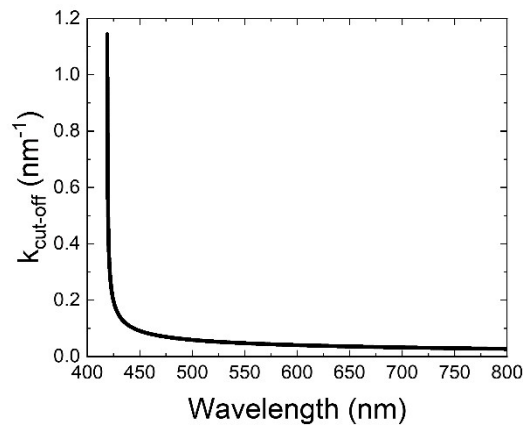


**Figure S4.** The calculated cut-off wave-vectors spectrum for the designed HMM structure.

### S4. The reflection spectra of the HMM and a 100 nm thick Ag film

The reflection measurements were performed using HMM and Ag film structures prepared on glass substrates and the incident light was incident on structure side. The obtained reflection spectra are summarized in Fig. S5.



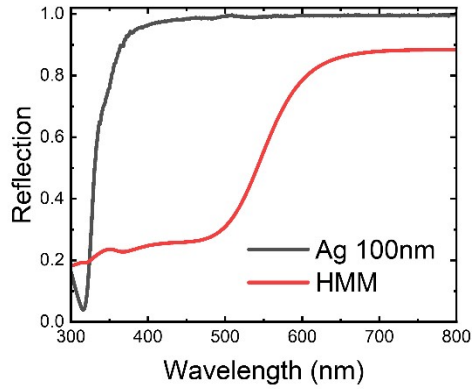


**Figure S5.** The reflection spectra of the HMM and a 100 nm thick Ag film on glass substrates.

**Supplemental references:**

- 1 C. L. Cortes, W. Newman, S. Molesky, and Z. Jacob, *J. Opt.*, 2012, **14**, 063001.
- 2 A. Poddubny, I. Iorsh, P. Belov, and Y. Kivshar, *Nat. Photonics*, 2013, **7**, 948.
- 3 L. Ferrari, J. S. T. Smalley, Y. Fainman, and Z. Liu, *Nanoscale*, 2017, **9**, 9034.
- 4 J. Gao, L. Sun, H. Deng, C. J. Mathai, S. Gangopadhyay, and X. Yang, *Appl. Phys. Lett.*, 2013, **103**, 051111.
- 5 A. Ghoshroy, W. Adams, X. Zhang, and DÖ Güney, *Phys. Rev. Appl.*, 2018, **10**, 024018.